ISSN 0976 – 3333

Available Online at www.ijpba.info

International Journal of Pharmaceutical & Biological Archives 2015; 6(2): 14 - 27

RESEARCH ARTICLE

A Study on Calibre Spectra of Nerve Fibres Innervating Intercostal and Extraocular Muscles in Selected Muscles of a Few Mammalian Species

M. Surendran, D. J. Prakash*

Postgraduate & Research Department of Zoology, Neurophysiology Unit, Voorhees College-632001, Tamilnadu, India

Received 24 Dec 2014; Revised 02 Apr 2015; Accepted 15 Apr 2015

ABSTRACT

Aim of the presnt study to evaluate the calibre spectra of nerve fibres Innervating Intercostal and Extraocular muscles in goat and squirrel. The animals used for the animal experiments belong to different mammalian orders as follows: Squirrel (Funambulas palmarum) Order–Rodentia; Goat–(Capra species) Order – Artiodactyla. The diameters of nerve fibres innervating the intercostal muscles and extraocular muscles and the importance of gamma and alpha motor nerve fibres in movements are described. A definite relationship may be established relating the prominent peak of small sized nerve fibres to the large number of muscle spindles. This may be expected to play appropriate role in both the thoracic region and eyes of goat and squirrel.

Key words: Intercostal muscles, Extraocular muscles,Goat, Motor nerve fibres and striated muscle.

1. INTRODUCTION

The fine movements of the hand in primates are controlled by the intrinsic muscles of the hand in close coordination with the extrinsic muscles. It is generally thought that the motor nerve fibres innervating muscles have bimodal calibre spectra. The thinner fibres (less than 6µm in diameter) are fusimotor and the larger fibres (greater than 8 µm in diameter) are skeletomotor. The diameters of nerve fibres are very important since the proper functioning of the entire system depends upon the velocity and frequencies of influence traffic in the peripheral nerves. The analysis of the fibre diameter composition of motor nerves is a reliable tool to study the organisation of the peripheral nervous system [1]. Introduced the concept of "motor unit', a unit consisting of a single motoneuron and the striated muscle fibres innervated by its axonal branches [2]**.** The motor units of higher primates appear to be the smallest in muscles like the small muscles of the hand, the laryngeal muscles and the extrinsic ocular muscles that are involved in fine differentiated movements. Such a small unit has nerve fibres of a finer calibre than larger ones [3]**.**

Bimodal size distribution:

Generally, in mammals, the motor nerve fibres fall into two groups when their calibre spectra are plotted. First, there are the large alpha motor or skeletomotor fibres (above about 8 µm diameter in the cat) which supply the extrafusal muscle fibres. Second, there are the smaller gamma motor fibres (below about 6 µm diameter in the cat) supplying the intrafusal fibres of the muscle spindles. Shneider et al., [4] were the first to establish the bimodal pattern in the deafferented limb muscles of the cat. The calibre spectra of the motor nerve fibres to the flexor and extensor muscles of the cat also showed a distinct bimodal distribution

Unimodal size distribution:

In contrast to the majority of the nerves supplying the limb muscles that are bimodal in distribution, the fibre composition of some muscle nerves shows a unimodal fibre size distribution [5]. Such muscle nerves with unimodal distribution were thought to have little or no proprioceptor supply [6]. However, motor nerves supplying the intrinsic hand muscles in the primate are not bimodal, yet these muscles are rich in muscle spindles [7].

Classification on the basis of conduction velocity:

***Corresponding Author:** Dr D J Prakash, **Email:** dejprakash@yahoo.co.in, **Phone No:** +91- 9443535112

IJPBA, Mar - Apr, 2015, Vol. 6, Issue, 2

The classification of nerve fibres on the morphological basis, inspired several investigators to provide the functional specializations of the two groups of nerve fibres. Mallik and Weir, [8], established that stimulation of the smaller motor nerve fibres resulted in an increase of nerve impulses in the sensory fibres. Manuel and Zytnicki [9] have elucidated the different functional roles of alpha and gamma motor fibres.

Studies of the compound action potentials also reveal two groups of myelinated motor nerve fibres based on different conduction velocities [10]. Spike potential size was an adequate criterion for identifying the activity of alpha and gamma motor fibres in limb muscle nerves. The large and small spikes are well differentiated and they may be assigned to groups of large and small diameter fibres. The existence of such grouping of the motor fibres can also be established histologically [11]. The proper use of these two motor pathways aids the nervous system in the precise execution of controlled movements.

Correlation between fibre diameter and conduction velocity:

The relation between the conduction velocity of myelinated nerve fibres and fibre diameter was first postulated by Gothlin. This view was later supported by various authors based on the work done [12]. Though the individual nerve fibres are subject to variation in diameter from level to level, the diameter of a nerve fibre is often estimated from its conduction velocity and in turn, fibre diameter is used to estimate fibre conduction velocity [13]. Such estimates have been reasonably good because the relationship is essentially linear. In man and monkey, in spite of their greater body size, the largest fibres are also slightly smaller and more slowly conducting than in the cat. The conduction velocity of both their largest motor and afferent fibres is below 90m/sec [14] In the present study to evualte the muscle spindle receptors of extraocular muscles in the squirrel and goat which, as it has been noted, are very striking in the non primates and which are very richly innervated in both cases/

2. MATERIALS AND METHODS

The nature of work done in this thesis deals with the organizational patterns related to the precise movements of certain muscles in mammals. It consists of a study of the caliber spectra of the first intercostals to twelfth thoracic ventral nerve roots innervating the intercostals and nerves to the extraocular muscles in species belonging to various mammalian orders.

Methodology for histological study of the composition of spinal ventral nerve roots and nerves innervating extrocular muscles.

The histological study aims to analyse the spectra of fibre diameters in the ventral roots at the first thoracic (T_1) to twelfth thoracic (T_{12}) levels and nerves to the eye muscles for the various mammalian species.

Animals

The animals used for the animal experiments belong to different mammalian orders as follows: Squirrel (*Funambulas palmarum*) Order– Rodentia; Goat–(*Capra species*) Order – Artiodactyla. The maturity of the animals was checked by noting the dentition. Only adult Male animals were used.

Dissection:

Nerves of extraocular muscles:

The eye lids and the skin surrounding the eye ball were incised; the skin was reflected to expose the walls of orbit. The orbital fat in which the eye ball is embedded was freed to expose the eyeball. The facial sheath was removed and the following nerves to eye muscles were dissected out. The Oculomotor nerve to inferior oblige and superior rectus, inferior rectus and medialis; The superior oblique supplying trochlear was removed.

Histological method

Fixation of the nerves and nerve roots:

The materials were fixed in 1% Osmium tetroxide. Since Osmium tetroxide is easily reduced [15], precaution was taken to use clean glasswares, free from all traces of organic solvents and finger prints.

Dehydration

After a week in Osmium tetroxide, the materials were washed twice with distilled water at intervals of one hour. They were then dehydrated using graded concentrations of ethyl alcohol (from 10%-70% in steps of 10%).

Measurement and counting of nerve fibres:

The slides were examined under a microscope (Carl Zeiss) and sections with perfect cross-sections were chosen for analysis. Photomicrographs were taken at a magnification of x100. Plate 1 and 2 show the specimen photomicrographs of the cross-sections of ventral roots and nerves.

3. RESULTS

Calibre spectra of nerve fibres innervating the left intercostal muscles

The results of the calibre spectra of nerve fibres innervating the Thoracic 1 intercostal muscles in mammals are shown in the tables (**Table 1,2,3 & 4**) and the (**Figure 1,2,3 & 4**) plotted as Histograms. The analysis of the calibre spectra of nerve fibres innervating the left and right intercostal muscles in Goat and Squirrel show the classical bimodal spectrum when graphs were plotted.

Calibre spectra of nerve fibres innervating the left intercostal muscles in squirrel:

The analysis of the calibre spectra of nerve fibres innervating the left intercostal muscles in Squirrel (Table 1 & Figure 1) show the classical bimodal spectrum.

Figure 1 A (T1 Lt) shows a clearly distinguishable peak in the range between 4 µm and 5 µm (76 fibres) and another peak in the range between 14 µm and 15 µm (78 fibres).

Figure 1 B (T2 Lt) displays a typical bimodal pattern with two peaks. A large peak comprising of small nerve fibres in the range between 5 µm and 6 µm (69 fibres) and a large peak in the range between 13 µm and 14 µm (67 fibres).

Figure 1 C (T3 Lt) depicts two prominent peaks; A peak in the range 4 µm and 5 µm (77 fibres) and a peak in the range 14 µm and 15 µm (68 fibres).

In Figure 1 D (T4 Lt) a gamma peak with small diameter nerve fibres at 5 µm – 6 µm (82 fibres) and a alpha peak with large diameter nerve fibres at 13 µm - 14 µm (66 fibres) are observed.

A dominant peak with gamma nerve fibres is seen in Figure 1 E (T5 Lt) in the range between 4 µm and 5 µm (79 fibres) and another prominent peak with alpha nerve fibres in the range between 13 µm and 14 µm (72 fibres).

Figure 1 F (T6 Lt) illustrates a bimodal pattern with two peaks; one at 5 µm - 6 µm (88 fibres) and another at 12 µm - 13 µm (71 fibres).

Similarly the results repeat two peaks in Figure 1 G. (T7 Lt). A large peak comprising of small nerve fibres in the range between 3 µm and 4 µm (96 fibres) and a large peak in the range between 13 µm and 14 µm (176 fibres).

In Figure 1 H (T8 Lt) a clear bimodal pattern is noticed. The small gamma nerve fibres are arranged in the range between 4 µm and 5 µm (108 fibres) and the large alpha nerve fibres are in the range between 13 µm and 14 µm (164 fibres).

Figure 1 I (T9 Lt) shows two peaks in the range between 4 µm and 5 µm (94 fibres) and between 14 µm and 15 µm (98 fibres).

Figure 1 J (T10 Lt) depicts the classical bimodal pattern of calibre spectra is seen at 5 µm - 6 µm (104 fibres) and at 14 µm - 15 µm (87 fibres).

The result shows two peaks in Figure 1 K (T11 Lt). A large peak comprising of small nerve fibres in the range between 4 µm and 5 µm (96 fibres) and a large peak in the range between 13 µm and 14 µm (97 fibres).

Figure 1 L (T12 Lt) depicts two dominant peaks; A peak in the range 4 µm and 5 µm (119 fibres) and a peak in the range 13 µm and 14 µm (98 fibres).

Calibre spectra of nerve fibres innervating the right intercostal muscles in squirrel:

The analysis of the calibre spectra of nerve fibres innervating the right intercostal muscles in Squirrel (Table 2 & Figure 2) show the classical bimodal spectrum.

A clearly observable prominent peak with gamma nerve fibres is seen in Figure 2 A (T1 Rt) in the range between 4 µm and 5 µm (124 fibres) and another prominent peak with alpha nerve fibres in the range between 14 µm and 15 µm (94 fibres).

Figure 2 B (T2 Rt) depicts two prominent peaks; A peak in the range 5 µm and 6 µm (99 fibres) and a peak in the range 14 µm and 15 µm (108 fibres).

Figure 2 C (T3 Rt) shows a clearly distinguishable peak in the range between 6 µm and 7 µm (101 fibres) and another peak in the range between 13 µm and 14 µm (124 fibres).

Figure 1 D (T4 Rt) displays a bimodal pattern with two peaks. A large peak comprising of small nerve fibres in the range between 5 µm and 6µm (117 fibres) and a large peak in the range between 15 µm and 16 µm (96 fibres).

A clearly observable prominent peak with gamma nerve fibres is seen in Figure 2 E (T5 Rt) in the range between 5 µm and 6 µm (91 fibres) and another prominent peak with alpha nerve fibres in the range between 13 µm and 14 µm (103 fibres).

In Figure 2 F (T6 Rt) a gamma peak with small diameter nerve fibres at 6 µm – 7 µm (109 fibres) and a alpha peak with large diameter nerve fibres at 13 µm – 14 µm (119 fibres) are observed.

Figure 2 G (T7 Rt) illustrates a bimodal pattern with two peaks; one at 3 µm - 4 µm (96 fibres) and another at 13 µm - 14 µm (107 fibres).

Similarly the results repeat two peaks in Figure 2 H (T8 Rt). A large peak comprising of small nerve fibres in the range between 5 µm and 6 µm (115 fibres) and a large peak in the range between 13 µm and 14 µm (113 fibres).

In Figure 2 I (T9 Rt) a distinguishable bimodal pattern is observed. The small gamma nerve fibres are arranged in the range between 4 µm and 5 µm (98 fibres) and the large alpha nerve fibres are in the range between 14 µm and 15 µm (92 fibres).

Figure 2 J (T10 Rt) shows two peaks in the range between 4 µm and 5 µm (115 fibres) and between 14 µm and 15 µm (103 fibres).

A noticeable bimodal pattern of calibre spectra is seen at 4 µm - 5 µm (128 fibres) and at 13 µm - 14 µm (119 fibres) in Figure 2 K (T11 Rt).

The results show two peaks in Figure 2 L (T12 Rt). A large peak comprising of small nerve fibres in the range between 5 µm and 6 µm (113 fibres) and a large peak in the range between 14 µm and 15 µm (93 fibres).

Calibre spectra of nerve fibres innervating the left intercostal muscles in goat

The analysis of the calibre spectra of nerve fibres innervating the left intercostal muscles in Goat (Table 3 & Figure 3) show the classical bimodal spectrum.

Figure 3 A (T1 Lt) shows a clearly distinguishable peak in the range between 4 µm and 5 µm (788 fibres) and another peak in the range between 13 µm and 14 µm (770 fibres).

Figure 3 B (T2 Lt) displays a bimodal pattern with two peaks. A large peak comprising of small nerve fibres in the range between 5 µm and 6 µm (755 fibres) and a large peak in the range between 12 µm and 13 µm (781 fibres).

Figure 3 C (T3 Lt) depicts two prominent peaks; A peak in the range 4 µm and 5 µm (795 fibres) and a peak in the range 14 µm and 15 µm (771 fibres).

In Figure 3 D (T4 Lt) a gamma peak with small diameter nerve fibres at 5 µm – 6 µm (895 fibres) and a alpha peak with large diameter nerve fibres at 15 µm - 16 µm (798 fibres) are observed.

A clearly observable prominent peak with gamma nerve fibres is seen in Figure 3 E. (T5 Lt) in the range between 3 µm and 4 µm (886 fibres) and another prominent peak with alpha nerve fibres in the range between 14 µm and 15 µm (829 fibres).

Figure 3 F (T6 Lt) illustrates a bimodal pattern with two peaks; one at 4 µm - 5 µm (784 fibres) and another at 13 µm - 14 µm (792 fibres).

Similarly the results repeat two peaks in Figure 3 G (T7 Lt) A large peak comprising of small nerve fibres in the range between 3 µm and 4 µm (883 fibres) and a large peak in the range between 15 µm and 16 µm (789 fibres).

In Figure 3 H (T8 Lt) a readily distinguishable bimodal pattern is noticed. The small gamma nerve fibres are arranged in the range between 4 µm and 5 µm (843 fibres) while the large alpha nerve fibres are in the range between 15 µm and 16 µm (996 fibres).

Figure 3 I (T9 Lt) shows two peaks in the range between 4 µm and 5 µm (968 fibres) and between 15 µm and 16 µm (1084 fibres).

A noticeable bimodal pattern of calibre spectra is seen at 3 µm - 4 µm (992 fibres) and at 14 µm - 15 µm (1072 fibres) in Figure 3 J (T10 Lt).

The results show two peaks in Figure 3 K (T11 Lt). A large peak comprising of small nerve fibres in the range between 4 µm and 5 µm (831 fibres) and a large peak in the range between 13 µm and 14 µm (1268 fibres).

Figure 3 L (T12 Lt) depicts two prominent peaks; A peak in the range 5 µm and 6 µm (904 fibres) and a peak in the range 15 µm and 16 µm (1053 fibres).

Calibre spectra of nerve fibres innervating the right intercostal muscles in goat:

The analysis of the measurement of nerve fibres innervating the right intercostal muscles in Goat show (Table 4 & Figure 4) the classical bimodal spectrum.

A clearly observable prominent peak with gamma nerve fibres is seen in Figure 4 A (T1 Rt) in the range between 4 µm and 5 µm (791 fibres) and another prominent peak with alpha nerve fibres in the range between 13 µm and 14 µm (785 fibres).

Figure 4 B (T2 Rt) depicts two prominent peaks; one peak in the range 4 - µm and 5 µm (779

fibres) and another peak in the range 13 µm and 14 µm (796 fibres).

Figure 4 C (T3 Rt) shows a clearly distinguishable peak in the range between 3 µm and 4 µm (792 fibres) and another peak in the range between 13 - µm and 14 µm (771 fibres).

Figure 4 D (T4 Rt) displays a bimodal pattern with two peaks. A large peak comprising of small nerve fibres in the range between 5 µm and 6 µm (789 fibres) and a large peak in the range between 13 µm and 14 µm (895 fibres).

A prominent peak with gamma nerve fibres is seen in Figure 4 E (T5 Rt) in the range between 3 µm and 4 µm (795 fibres) and another prominent peak with alpha nerve fibres in the range between 13 µm and 14 µm (757 fibres).

In Figure 4 F (T6 Rt) a gamma peak with small diameter nerve fibres at 5 µm – 6 µm (787 fibres) and a alpha peak with large diameter nerve fibres at 13 µm – 14 µm (776 fibres) are observed.
Figure 4 G (T7 Rt) illustrates a bimodal pattern with two peaks; one at 3 µm - 4 µm (795 fibres) and another at 14 µm - 15 µm (791 fibres).

Similarly the results repeat two peaks in Figure 4 H (T8 Rt). A large peak comprising of small nerve fibres in the range between 4 µm and 5 µm (732 fibres) and a large peak in the range between 15 µm and 16 µm (783 fibres).

In Figure 4 I (T9 Rt) a readily distinguishable bimodal pattern is noticed. The small gamma nerve fibres are arranged in the range between 4 µm and 5 µm (788 fibres) and the large alpha nerve fibres are in the range between 12 µm and 13 µm (788 fibres).

Figure 4 J (T10 Rt) shows two peaks in the range between 3 µm and 4 µm (757 fibres) and between 13 µm and 146 µm (796 fibres).

A typical bimodal pattern of calibre spectra is seen at 5 µm - 6 µm (785 fibres) and at 13 µm - 14 µm (769 fibres) in Figure 4 K (T11 Rt).

The result shows two peaks in Figure 4 L (T12 Rt). A large peak comprising of small nerve fibres in the range between 4 µm and 5 µm (771 fibres) while a large peak in the range between 14 µm and 15 µm (732 fibres).

Calibre spectra of nerve fibres innervating the extraocular muscles

The results of the calibre spectra of nerve fibres innervating the left and right extraocular muscles in Squirrel and Goat are shown in the tables (**Table 5,6,7 & 8**) and the (**Figures 5,6,7 & 8**) plotted as Histograms.

The analysis of the calibre spectra of nerve fibres innervating the left and right extraocular muscles in Squirrel and Goat show the classical bimodal spectrum when graphs were plotted (Table 5-8 and Figure 5-8).

Calibre spectra of nerve fibres innervating the left extraocular muscles in squirrel:

A noticeable bimodal distribution pattern of Oculomotor superior branch of left extraocular muscles in Squirrel. A peak is observed in Figure 5 A in the range between 4 µm and 5 µm (24 fibres) and 15 µm and 16 µm (21 fibres) with a dip in the range between 7 µm and 8 µm (3 fibres).

Similarly, the results of fibre analysis of left Oculomotor inferior branch in Squirrel shows two peaks, one in the range between 4 µm and 5 µm (31 fibres) and another peak in the range between 14 µm and 15 µm (28 fibres) with a division point in the range 7 µm – 8 µm (4 fibres) in Figure 5 B.

In Figure 5 C, the left Abducens depicts a pattern comprising of a small peak with 29 fibres in the range between 4 µm and 5 µm and 26 fibres in the range 14 µm and 15 µm with a dip in the range 7 µm - 8 µm (3 fibres).

Figure 5 D shows a bimodal pattern; one peak predominantly comprising of small nerve fibres is observed in the range 5 µm and 6 µm (30 fibres) and large fibres constituting another peak in the range between 16 µm and 17 µm (32 fibres) with division point in the range 8 µm and 9 µm (3 fibres).

Calibre spectra of nerve fibres innervating the right extraocular muscles in squirrel:

The fibre analysis of right Oculomotor superior branch of extraocular muscle in Squirrel shows a clearly distinguishable prominent peak with small nerve fibres in Figure 6 A in the range between 4 µm and 5 µm (21 fibres) and another prominent peak with larger nerve fibres in the range between 15 µm and 16 µm (24 fibres) with a dip in the range 7 µm - 8 µm (5 fibres).

The fibre distribution pattern of right Oculomotor inferior branch shows a clearly distinguishable prominent peak with small nerve fibres in Figure 6 B in the range between 5 µm and 6 µm (22 fibres) and another prominent peak with larger

nerve fibres in the range between 14 µm and 15 µm (29 fibres) with a dip in the range 7 µm - 8 µm (2 fibres).

Similarly, the results of fibre analysis of right Trochlear branch in Squirrel shows two peaks, one in the range between 6 µm and 7 µm (31 fibres) and another peak in the range between 15 µm and 16 µm (34 fibres) with a division point in the range 9 µm – 10 µm (3 fibres) in Figure.6.C.

A noticeable bimodal distribution pattern of right Abducens branch of extraocular muscles in Squirrel is observed in Figure 6 D in the range between 5 µm and 6 µm (24 fibres) and 16 µm and 17 µm (31 fibres) with a dip in the range between 8 µm and 9 µm (2 fibres).

Calibre spectra of nerve fibres innervating the left extraocular muscles in goat:

The fibre analysis of the left Oculomotor superior branch in Goat shows a clearly distinguishable prominent peak with small nerve fibres in Figure 7 A in the range between 4 µm and 5 µm (41 fibres) and another prominent peak with larger nerve fibres in the range between 14 µm and 15 µm (46 fibres) with a dip in the range 7 µm - 8 µm (8 fibres).

Figure 7 B shows a calibre spectrum of left Oculomotor inferior branch with a large peak comprising of small fibres in the range 4 µm - 5 µm (31 fibres) and another peak with large fibres in the range 13 µm - 14 µm (48 fibres) with a division point in the range 8 µm - 9 µm (2 fibres).

The left Trochlear nerve displays two peaks in Figure 7 C; One in the range between 5 µm and 6 µm (35 fibres) and the other peak in the range between 13 µm and 14 µm (47 fibres) with a dip in the range between 8 µm and 9 µm (3 fibres).

In Figure 7 D, a clear bimodal pattern is observed in left Abducens nerve. Small fibres constitute a peak in the range 6 µm to 7 µm (47 fibres) and large fibres in the range 15 µm - 16 µm (41 fibres). The division point is noted in the range 9 µm - 10 µm (4 fibres).

Calibre spectra of nerve fibres innervating the right extraocular muscles in goat:

The right Oculomotor superior branch of right extraocular muscles in Goat displays two peaks in Figure 8 A; One peak in the range between 4 µm and 5 µm (37 fibres) and the other peak in the range between 14 µm and 15 µm (42 fibres) with a dip in the range between 7 µm and 8 µm (6 fibres).

The fibre distribution pattern of right Oculomotor inferior branch shows a clearly distinguishable prominent peak with small nerve fibres in Figure 8 B in the range between 4µm and 5µm (22 fibres) and another prominent peak with larger nerve fibres in the range between 15 µm and 16 µm (46 fibres) with a dip in the range 8 µm - 9 µm and 9 µm - 10 µm (4 fibres).

Figure 8 C shows a calibre spectrum of right Trochlear branch with a large peak comprising of small fibres in the range 5 µm - 6 µm (36 fibres) and another peak with large fibres in the range 13 µm - 14 µm (35 fibres) with a division point in the range 7 µm - 8 µm (10 fibres).

Figure 8 D illustrates the fibre distribution pattern of right Abducens branch with a large peak comprising of small fibres in the range 5 µm - 6 µm (22 fibres) and another peak with large fibres in the range 16 µm - 17 µm (35 fibres) with a division point in the range 8 µm - 9 µm and 9 µm - 10 µm (4 fibres).

Table 1: Calibre spectra of myelinated nerve fibres innervating the left intercostals muscles in squirrel

Diameter (µm) / Nerve	0-1	1-2	2-3	3-4	4-5	5-6	6-7	7-8	8-9	9-10	10-11	11-12	12-13	13-14	14-15	15-16	16-17	17-18	18-19	19-20	20-21	Total
T1	0	7	12	18	76	69	51	49	36	28	18	12	74	64	78	58	48	37	31	29	16	811
T2	0	5	40	45	64	69	75	46	38	33	29	38	78	67	69	56	51	46	38	30	17	934
T3	0	4	9	68	77	72	71	66	58	49	37	26	76	65	68	57	47	38	23	18	15	944
T4	0	7	42	46	68	82	70	55	46	34	30	29	69	66	7	64	52	48	37	32	18	902
T5	0	6	18	15	79	70	64	57	49	41	39	30	26	72	69	58	47	39	25	19	16	839
T6	0	8	41	45	62	88	74	57	47	36	31	28	71	66	63	68	53	49	39	36	19	981
T7	0	7	29	96	63	58	43	39	32	24	19	71	67	176	88	49	36	30	26	19	16	988
T8	0	6	37	71	108	61	59	46	39	35	33	38	69	164	99	54	55	48	39	36	28	1125
T9	0	5	28	38	94	69	54	41	34	26	11	8	58	77	98	40	37	31	28	18	14	809
T10	0	9	41	43	69	104	78	52	49	36	24	17	65	73	87	56	53	47	37	35	19	994
T11	0	14	26	39	96	81	75	54	46	38	31	29	67	97	78	51	46	32	29	22	18	969
T12	0	8	39	44	119	95	68	53	41	37	25	18	75	98	65	54	52	48	38	35	26	1038

Table 2: Calibre spectra of myelinated nerve fibres innervating the right intercular muscles in squirrel

Diameter (µm) / Nerve	0-1	1-2	2-3	3-4	4-5	5-6	6-7	7-8	8-9	9-10	10-11	11-12	12-13	13-14	14-15	15-16	16-17	17-18	18-19	19-20	20-21	Total
T1	0	14	29	36	124	88	77	59	42	36	28	16	59	86	94	72	54	45	31	28	18	1036
T2	0	5	40	46	73	99	67	56	48	37	22	13	67	86	108	74	35	31	27	23	18	975
T3	0	16	31	47	59	82	101	72	48	41	39	32	78	124	97	88	46	41	38	32	29	1141

T4	0	7	41	48	89	117	68	47	35	37	45	54	60	67	79	96	53	42	40	38	28	1091
T5	0	18	36	41	73	91	66	52	49	42	34	74	76	103	88	64	42	38	31	29	24	1071
T6	0	14	42	51	61	87	109	55	48	41	37	61	86	119	72	52	48	42	36	31	12	1104
T7	0	5	42	96	77	65	56	48	35	27	18	14	64	107	83	63	47	36	29	19	16	947
T8	0	2	41	68	89	115	70	49	36	39	48	66	87	113	75	58	47	57	42	35	25	1162
T9	0	4	13	67	98	74	53	49	37	24	21	19	61	68	92	75	41	27	20	16	8	867
T10	0	5	41	89	115	92	69	50	37	41	46	67	68	80	103	78	43	56	43	38	17	1178
T11	0	7	14	78	128	93	69	31	26	26	15	10	75	119	63	44	39	21	20	18	9	905
T12	0	6	41	51	97	113	81	52	40	43	48	66	79	80	96	83	64	58	46	40	18	1202

Table 3: Calibre spectra of myelinated nerve fibres innervating the left intercostals muscles in goat

Diameter (µm) / **Nerve**	**0-1**	**1-2**	**2-3**	**3-4**	**4-5**	**5-6**	**6-7**	**7-8**	**8-9**	**9-10**	**10-11**	**11-12**	**12-13**	**13-14**	**14-15**	**15-16**	**16-17**	**17-18**	**18-19**	**19-20**	**20-21**	**Total**
T1	0	95	364	761	788	694	515	481	454	392	368	317	758	770	743	688	655	563	547	436	385	10774
T2	0	76	408	603	652	755	570	461	382	343	266	217	781	705	708	655	572	488	426	354	256	9738
T3	0	126	452	639	795	640	523	512	496	458	419	366	697	724	771	641	615	576	521	475	363	10809
T4	0	153	479	615	667	895	625	562	517	483	441	397	741	633	675	798	675	526	471	445	382	11180
T5	0	164	393	886	768	684	540	461	415	355	314	272	645	712	829	731	669	612	561	528	457	10996
T6	0	187	292	667	784	779	715	663	617	573	528	493	718	792	774	752	741	611	567	519	463	12235
T7	0	94	298	883	765	746	712	653	562	473	419	377	322	726	709	789	761	698	627	588	516	11718
T8	0	116	351	722	843	736	714	626	574	519	466	447	353	773	996	742	694	556	519	477	426	11650
T9	0	164	319	734	968	781	726	661	639	577	529	485	381	688	753	1084	732	672	618	564	437	12512
T10	0	141	346	992	762	699	644	547	471	452	366	292	177	793	1072	659	686	568	519	467	389	11042
T11	0	188	469	595	831	777	718	641	571	408	355	317	261	1268	739	666	781	683	616	533	464	11881
T12	0	211	376	758	791	904	672	556	492	429	374	310	278	741	719	1053	614	544	478	412	358	11070

Table 4: Calibre spectra of myelinated nerve fibres innervating the right intercostals muscles in goat

Diameter (µm) / **Nerve**	**0-1**	**1-2**	**2-3**	**3-4**	**4-5**	**5-6**	**6-7**	**7-8**	**8-9**	**9-10**	**10-11**	**11-12**	**12-13**	**13-14**	**14-15**	**15-16**	**16-17**	**17-18**	**18-19**	**19-20**	**20-21**	**Total**
T1	0	86	211	659	791	715	642	616	561	522	477	424	769	785	644	581	532	489	378	326	292	10500
T2	0	146	294	712	779	681	545	488	443	358	316	259	667	796	744	608	546	462	419	353	273	9889
T3	0	194	241	792	754	703	656	619	533	476	411	371	728	771	694	616	574	514	486	457	381	10971
T4	0	231	353	668	764	789	544	461	409	367	319	242	710	895	687	622	585	534	458	418	349	10405
T5	0	181	268	795	744	686	616	549	507	441	372	321	655	757	695	617	574	511	462	402	355	10508
T6	0	162	386	749	669	787	631	557	463	415	341	312	737	776	647	585	528	499	442	391	315	10392
T7	0	63	216	795	644	771	607	582	452	430	396	275	768	727	791	668	531	574	481	418	351	10540
T8	0	97	418	446	732	689	711	658	574	521	486	455	393	702	753	783	508	448	371	295	193	10233
T9	0	155	296	692	788	715	619	574	463	355	284	182	788	748	694	581	466	352	324	309	243	9628
T10	0	82	391	757	710	695	575	479	417	332	286	435	682	796	665	563	512	457	368	304	182	9688
T11	0	67	115	643	726	785	614	583	520	502	496	375	260	769	711	651	547	461	334	292	254	9707
T12	0	77	358	461	771	715	568	551	421	347	288	448	622	691	732	574	521	478	341	311	196	9471

Table 5: Calibre spectra of myelinated nerve fibres innervating left extraocular muscles in Squirrel

Diameter (µm) / **Nerve**	**0-1**	**1-2**	**2-3**	**3-4**	**4-5**	**5-6**	**6-7**	**7-8**	**8-9**	**9-10**	**10-11**	**11-12**	**12-13**	**13-14**	**14-15**	**15-16**	**16-17**	**17-18**	**18-19**	**19-20**	**20-21**	21-22	22-23	23-24	Total numbers of nerve fibers
OSB	0	1	7	11	24	9	7	3	9	9	14	16	18	18	20	21	12	5	3	2	2	0	0	0	211
OIB	0	2	4	15	31	12	4	4	7	11	12	19	21	23	28	13	9	4	2	1	1	0	0	0	223
Trochlear	0	2	5	13	29	12	3	3	5	9	9	15	18	21	26	14	10	3	2	2	1	0	0	0	202
Abducens	0	2	3	11	24	30	15	4	3	8	15	18	18	21	24	29	32	15	8	3	2	1	0	0	286

Table 6: Calibre spectra of myelinated nerve fibres innervating right extraocular muscles in Squirrel

Diameter (µm) / Nerve	**0-1**	**1-2**	**2-3**	**3-4**	**4-5**	**5-6**	**6-7**	**7-8**	**8-9**	**9-10**	**10-11**	**11-12**	**12-13**	**13-14**	**14-15**	**15-16**	**16-17**	**17-18**	**18-19**	**19-20**	**20-21**	21-22	22-23	23-24	Total numbers of nerve fibers
OSB	0	2	4	9	21	12	9	5	8	10	13	17	16	17	17	24	9	4	2	2	1	0	0	0	202
OIB	0	0	5	11	19	22	17	2	3	7	12	16	19	21	29	18	12	9	8	4	2	2	0	0	238
Trochlear	0	1	2	7	15	27	31	11	6	3	8	17	21	25	30	34	16	7	4	3	2	2	1	0	273
Abducens	0	0	3	7	21	24	18	3	2	8	11	17	20	22	24	31	15	10	9	7	3	2	1	0	258

Table 7: Calibre spectra of myelinated nerve fibres innervating left extraocular muscles in goat

Diameter (µm) / **Nerve**	**0-1**	**1-2**	**2-3**	**3-4**	**4-5**	**5-6**	**6-7**	**7-8**	**8-9**	**9-10**	**10-11**	**11-12**	**12-13**	**13-14**	**14-15**	**15-16**	**16-17**	**17-18**	**18-19**	**19-20**	**20-21**	21-22	22-23	23-24	Total numbers of nerve fibers
OSB	0	2	17	22	41	19	13	8	16	21	27	32	37	42	46	17	12	8	8	3	2	0	0	0	393
OIB	0	3	9	14	31	28	17	6	2	18	22	27	33	48	31	29	15	7	3	1	0	0	0	0	344
Trochlear	0	2	7	15	24	35	17	7	3	20	24	29	31	47	30	25	14	3	3	2	1	0	0	0	339
Abducens	0	2	9	17	25	31	42	29	17	4	9	15	21	30	37	41	19	13	7	2	1	0	0	0	371

Table 8: Calibre spectra of myelinated nerve fibres innervating right extraocular muscles in goat

Diameter (µm) / **Nerve**	**0-1**	**1-2**	**2-3**	**3-4**	**4-5**	**5-6**	**6-7**	**7-8**	**8-9**	**9-10**	**10-11**	**11-12**	**12-13**	**13-14**	**14-15**	**15-16**	**16-17**	**17-18**	**18-19**	**19-20**	**20-21**	21-22	22-23	23-24	Total numbers of nerve fibers
OSB	0	1	11	18	37	21	14	6	13	18	20	24	29	33	42	34	9	8	5	2	2	2	0	0	349
OIB	0	2	7	9	22	13	7	5	4	4	11	16	17	21	27	46	12	9	8	4	1	0	0	0	245
Trochlear	0	1	8	15	21	36	22	10	15	15	20	23	27	35	30	17	9	6	4	2	1	1	0	0	320

Abducens	0	1	1	4	17	22	15	10	4	4	12	17	21	24	27	29	35	21	15	7	2	1	1	0	290

FIGURE.1
Histogram showing the distribution pattern of Myelinated nerve fibres innervating Left intercostal muscles in Squirrel.

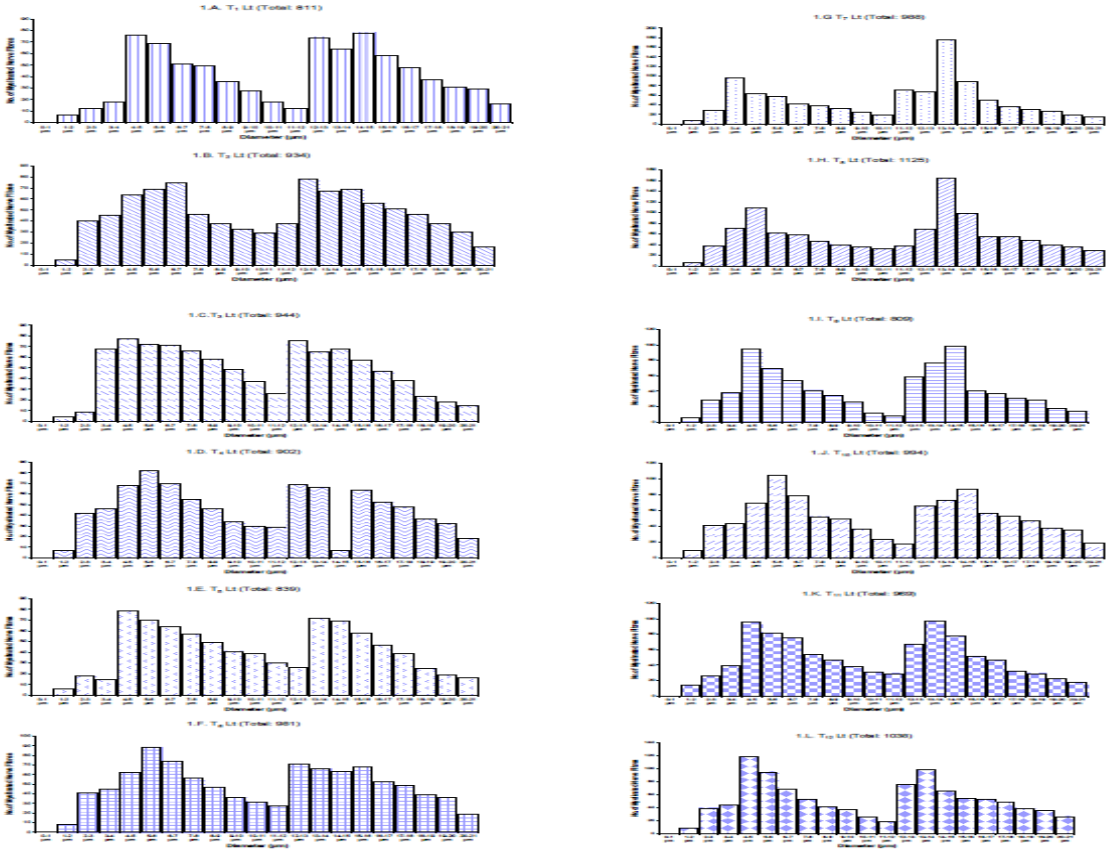

FIGURE.2
Histogram showing the distribution pattern of Myelinated nerve fibres innervating Right intercostal muscles in Squirrel.

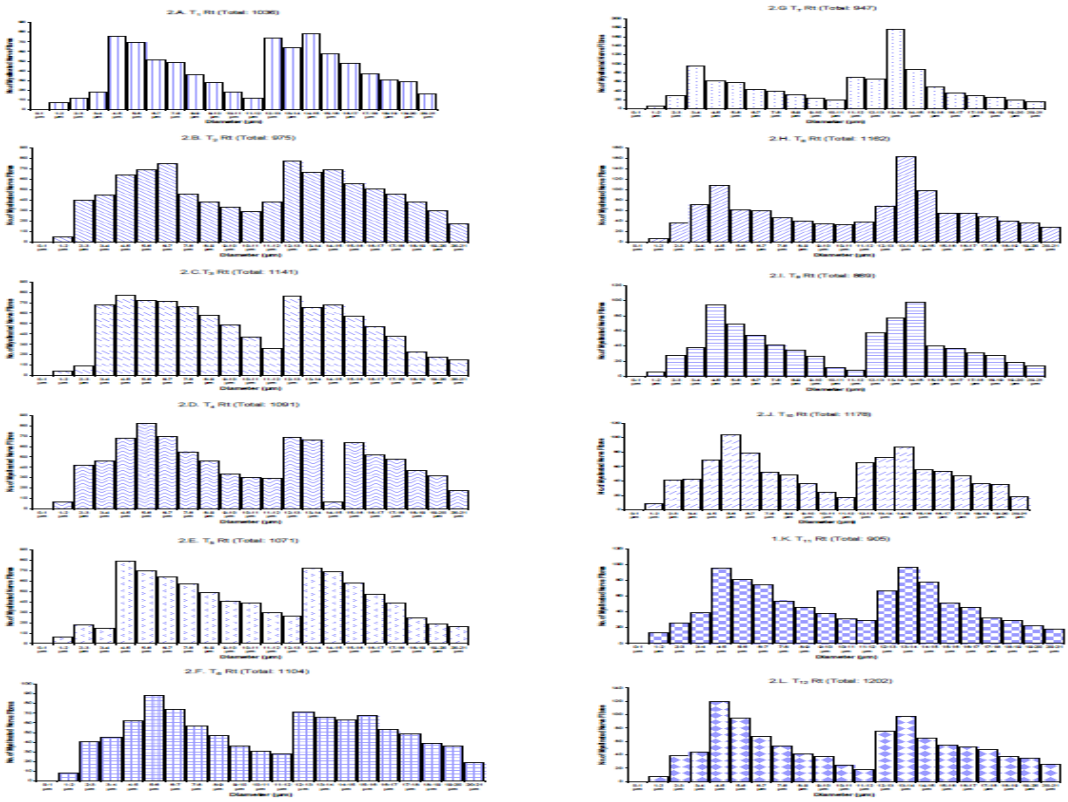

FIGURE.3
Histogram showing the distribution pattern of Myelinated nerve fibres innervating Left intercostal muscles in Goat.

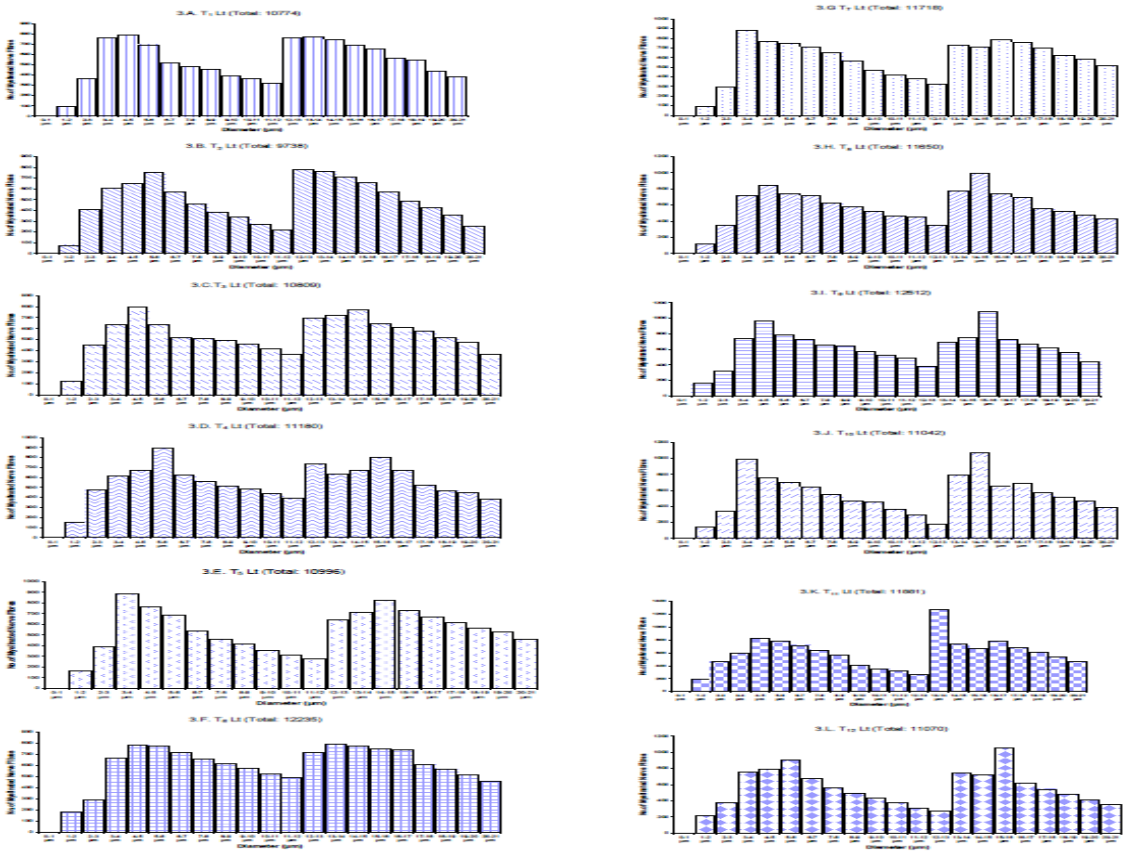

FIGURE.4
Histogram showing the distribution pattern of Myelinated nerve fibres innervating Right intercostal muscles in Goat.

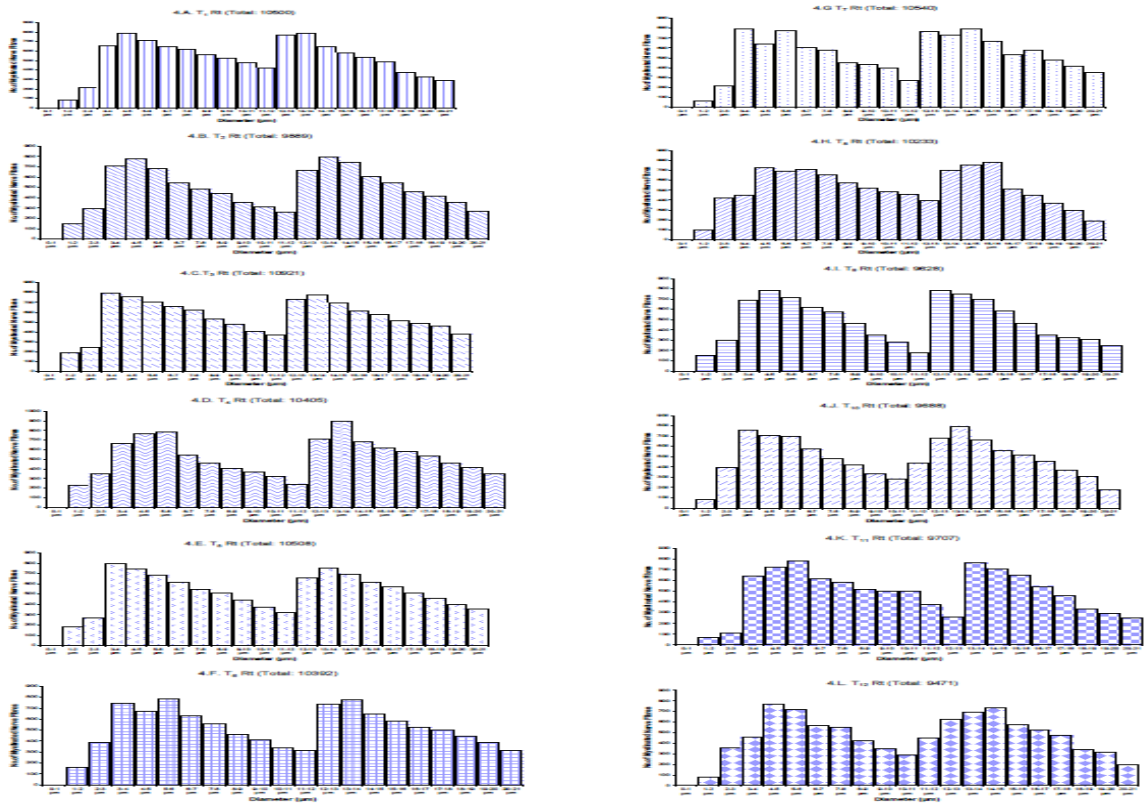

IJPBA, Mar - Apr, 2015, Vol. 6, Issue, 2

FIGURE.5
Histogram showing the distribution pattern of Myelinated nerve fibres innervating Left extraocular muscles in Squirrel.

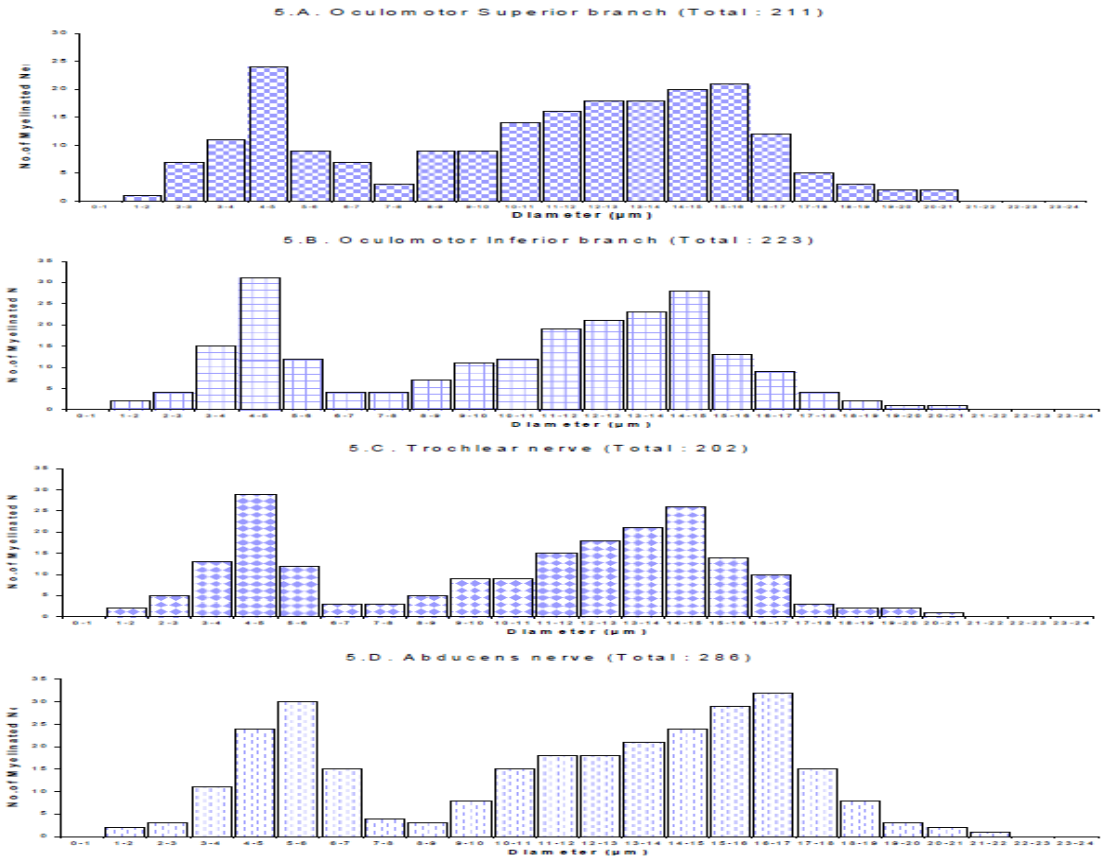

FIGURE.6
Histogram showing the distribution pattern of Myelinated nerve fibres innervating Right extraocular muscles in Squirrel.

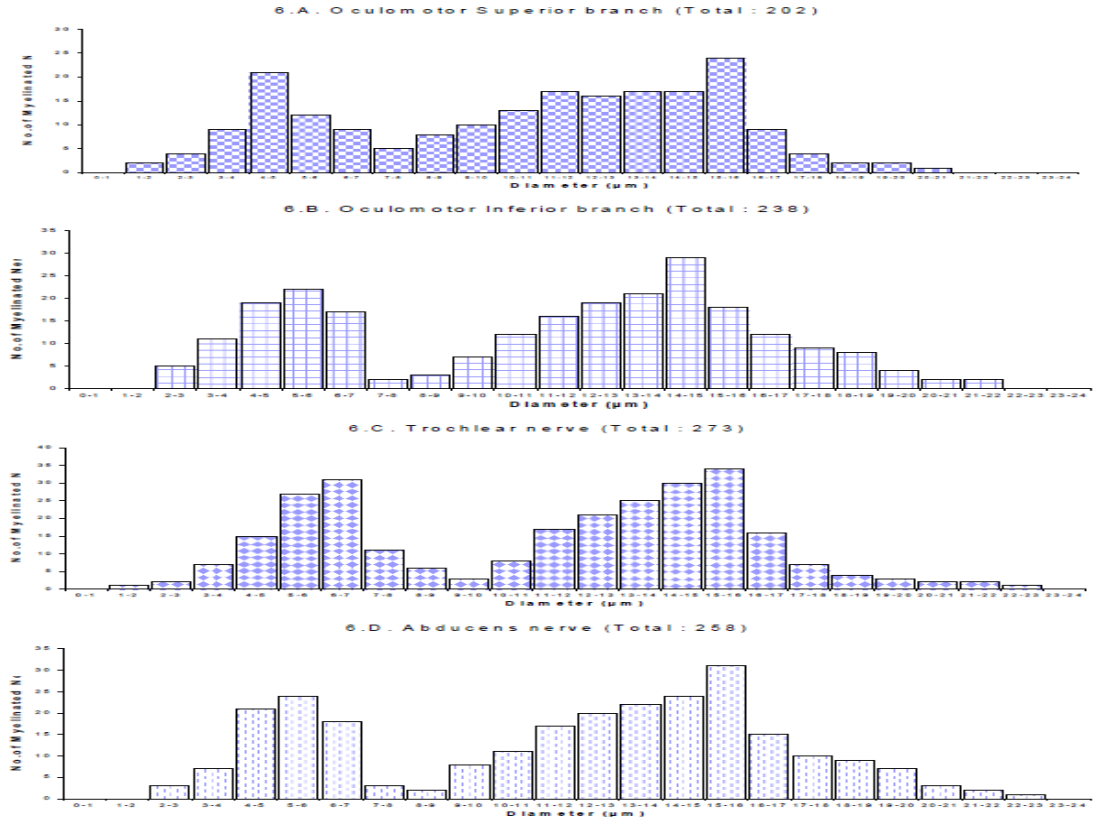

FIGURE.7
Histogram showing the distribution pattern of Myelinated nerve fibres innervating Left extraocular muscles in Goat.

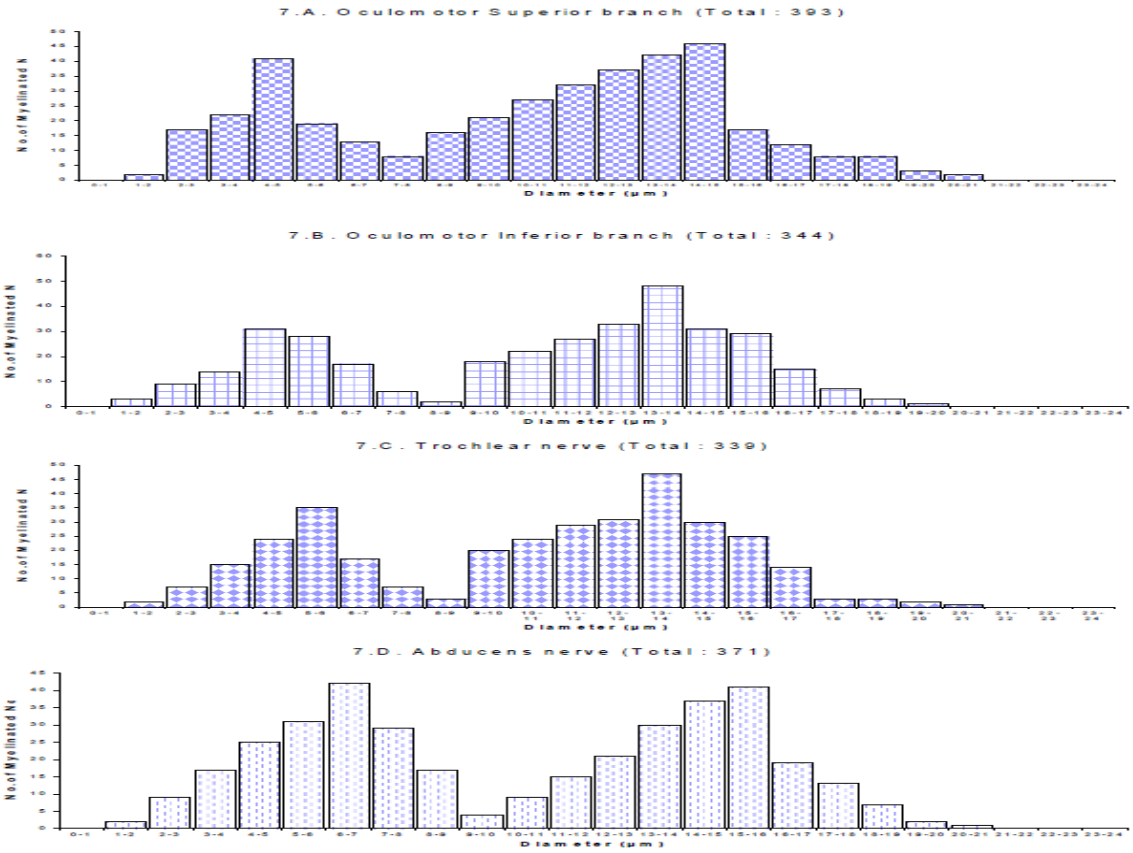

FIGURE.8
Histogram showing the distribution pattern of Myelinated nerve fibres innervating Right extraocular muscles in Goat.

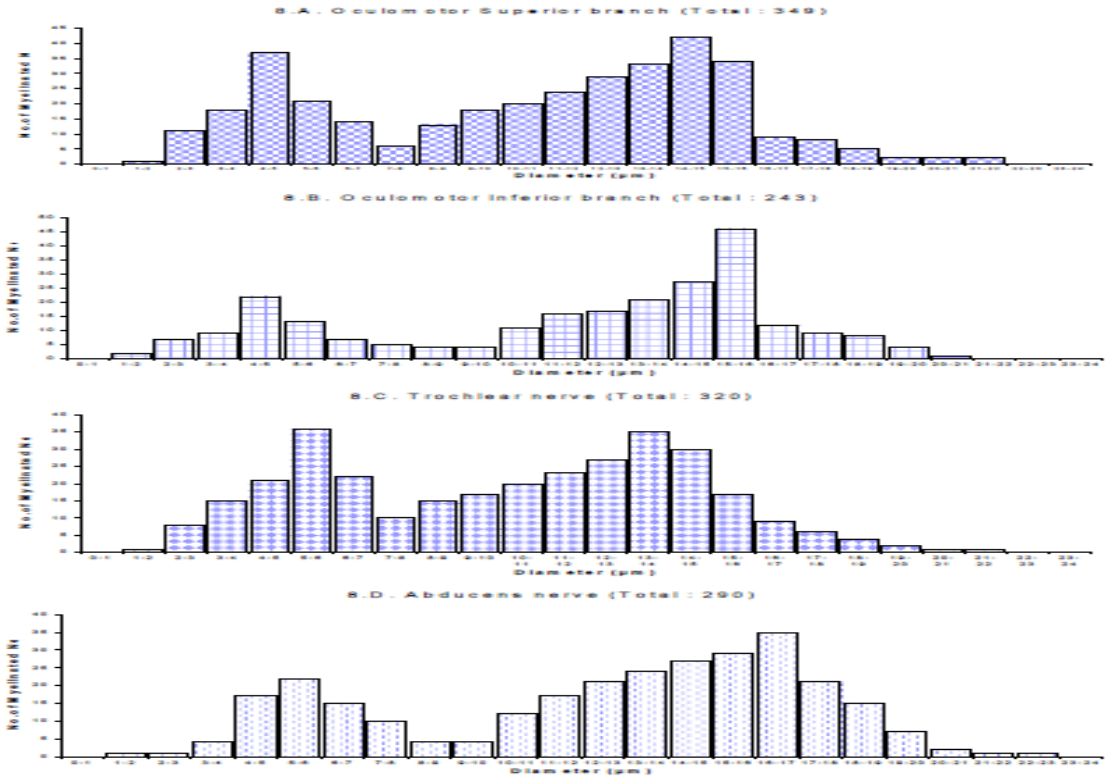

4. DISCUSSION

Bimodal calibre spectra of motor nerve fibres innervating the limb muscles are generally found in mammals [16]. The functions of the limbs are, so multitudinously various. The course of the nerve fibres gives important information as to the morphological arrangement of the structure of the limb. Therefore, the individual spinal neurons, innervating a particular muscle, their co-ordinate action and synchronous discharge depends on some physiology quality common to all. However, such a typical bimodal pattern was not found in the motor fibres of the deep ulnar nerve of the bonnet monkey [17]. The present work was undertaken in order to observe the nature of the distribution pattern of the nerve fibre size in the thoracic ventral nerve roots innervating the intercostal muscles and the nerves supplying the eye muscles in squirrel and goat.

From the results, the typical bimodal nature of distribution of nerve fibres with clear gamma and alpha peaks is obtained in squirrel and goat. Following the physiological demonstration, that in the cat, the γ efferent fibres are exclusively devoted to supplying muscle spindles, it tended to be assumed that all the plate endings were derived from the branches of γ fibres. The muscles of the neck, head and intercostal muscles can be very rich in muscles spindles. The small muscles of the hand involved in the fine, precise and manipulative movements contain dense concentrations of muscle spindles [18]. The ventral roots should contain many fusimotor nerve fibres exhibit bimodal pattern when their calibre spectra are plotted.

While bimodality is not an uncommon among mammals, some animals do not exhibit such a classical pattern. The distribution is not bimodal in shrew, monkey, squirrel and rabbit [19] in their calibre spectra of nerve fibres innervating the muscles of the forelimb. This suggests that a separation into small fibres (gamma) and large fibres (alpha) on the basis of fibre diameter is not found in all mammals. Such a separation should have evolved at some stage of evolution, i.e. after the evolution of rodents.

The overlapping of the gamma and alpha groups of nerve fibres necessarily reflect in the conduction velocity. Such an overlap in the electroneurogram suggests the possibility of beta fibres [20]. The identification of fusimotor in the above animals based on fibre diameter is not possible. This is because, the primates use their hands for specialized, prehensile movements, whereas the rodents, the unspecialized mammals that use forelimbs for handling food**.** Such a functional difference applies to the intercostal muscles also. The distribution of motor fibres in the intercostal nerves of the cat is markedly bimodal. The coordinated and concerted activity of the extrinsic and intrinsic musculature of the intercostal muscles results in a variety of precise manipulative movements. The ribs of the thoracic basket are highly mobile such that even finely changes in the muscular forces would result in appreciable changes in the position of the ribs. Such a need for accuracy in the intercostal movements necessitates a very tight regulation of peripheral control mechanisms.

However, there should not seem to be any noteworthy difference between the various mammalian species with reference to inspiratory and expiratory activities of the interecostal muscles [21]. The principal inspiratory muscles are thus the diaphragm and the interchondrals. All the same the superior, external intercostals may present a typical inspiratory activity. The experimental results obtained [22], suggest that the intercostal motoneurons innervated by the thoracic spinal nerves are under the influence of the respiratory centre.

The distribution of motor fibres in the intercostal nerves of the cat is markedly bimodal [23]. The coordinated and concerted activity of the extrinsic and intrinsic musculature of the intercostal muscles results in a variety of precise manipulative movements [24]. The ribs of the thoracic basket are highly mobile such that even finely changes in the muscular forces would result in appreciable changes in the position of the ribs. Such a need for accuracy in the intercostal movements necessitates a very tight regulation of peripheral control mechanisms. The results have prompted to consider the external and internal intercostals as particular postural muscles.

The extraocular muscles of most of vertebrates that have been examined do not contain muscle spindles but the eye muscles of a few do. Naively, one might have supposed that the presence of the most sophisticated, centrally adjustable, muscle receptor would be associated with the widest range and greatest complexity of eye movement innervated by cluster of small myelinated nerve fibres. Thus, although some afferent discharges paused during an extrafusal contraction, most showed a more complicated response which

varied with the strength of the extrafusal contraction. During minimal extrafusal contractions they were excited, at slightly higher strengths unloaded, and during maximal contractions they were again excited.

Therefore the present study shows the bimodal pattern of nerve fibre distribution indicating the rich population of muscle spindles. A definite relationship may be established relating the prominent peak of small sized nerve fibres to the large number of muscle spindles. This may be expected to play appropriate role in both the thoracic region and eyes of squirrel and goat.

CONCLUSION

Further study of the nerve fibre distribution may be continued, involving the morphometric analysis of muscle spindles such as the measurement, number, density and distribution in order to understand the functional organization.

REFERENCES

1. Mochizuki, Y., Tanaka, H., Matsumoto, K., Sano, H., Toki, H., Shimoura, H., Ooka, J., Sawa, T., Motoji, Y., Ryo, K., Hirota, Y., Ogawa, W., Hirata, K. (2015). Association of peripheral nerve conduction in diabetic neuropathy with subclinical left ventricular systolic dysfunction. *Cardiovascular Diabetology*. 14:47.
2. Vishram Singh. (2014). Textbook of Clinical Neuroanatomy. Elsevier Health Sciences. Medical.Pages-268.
3. Smith, C. (2008). Biology of Sensory Systems. John Wiley & Sons, Medical. Pages- 534.
4. Shneider, N.A., Brown, M.N., Smith, C.A., Pickel, J., Alvarez, F.J., (2009). Gamma motor neurons express distinct genetic markers at birth and require muscle spindle-derived GDNF for postnatal survival. Neural Dev. 4: 42.
5. Bilego Neto, A.P.C., Cassiano Silveira, F.B., Rodrigues da Silva, G.A., Sayuri Sanada, L., Sassoli Fazan, V.P. (2013). Reproducibility in Nerve Morphometry: Comparison between Methods and among Observers. BioMed Res Int. 1-7.
6. Brushart, T.M. (2011). Nerve Repair. Oxford University Press, USA, Medical.P-480
7. Wang, K., McGlinn, E.P., Chung, K.C. (2014). A biomechanical and evolutionary perspective on the function of the lumbrical muscle. J Hand Surg Am. 39(1):149-55.
8. Mallik, A., Weir, A.I. (2005). Nerve conduction studies: essentials and pitfalls in practice. J Neurol Neurosurg Psychiatry. 76.
9. Manuel, M., Zytnicki, D. (2011). Alpha, beta and gamma motoneurons: functional diversity in the motor system's final pathway. J Integr Neurosci. 10(3):243-76.
10. Jun Kimura, 2001. Electrodiagnosis in Diseases of Nerve and Muscle : Principles and Practice: Principles and Practice. Oxford University Press, USA, Medical. Pages-1024.
11. Swash, M., Schwartz, M.S. (2013). Neuromuscular Diseases: A Practical Approach to Diagnosis and Management. Springer Science & Business Media. Medical - 456 pages.
12. Ikeda, Oka. (2012). The relationship between nerve conduction velocity and fiber morphology during peripheral nerve regeneration. Brain Behav. 2(4): 382–390.
13. Beck, R. (2006). Muscle Fiber Conduction Velocity. Biomedical Engineering, General & Introductory Biomedical Engineering, Wiley Encyclopedia of Biomedical Engineering.
14. Galan, F., Baker, S.N. (2014). Pre-synaptic inhibition of afferent feedback in the macaque spinal cord does not modulate with cycles of peripheral oscillations around 10 Hz.bioRxiv.
15. Robinson, G. (1982). Electron microscopy 2: Transmission (A) Tissue preparation; (B) Sectioning and staining. 482-518. In : Theory and practice of histological techniques. (Eds) Bancroft, J.D. and Stevens, A. Churchill Livingstone Edinburg.
16. Schiaffino, S., Reggiani, C. (2011). Fiber Types in Mammalian Skeletal Muscles. Physiological Reviews. 91(4): 1447-1531
17. Oguzhanoglu, A., Guler, S., Cam, M., Degirmenci, E. (2010). Conduction in ulnar nerve bundles that innervate the proximal and distal muscles: a clinical trial. BMC Neurol. 10:81.
18. Palastanga, N., Field, D., Soames, R.W. (2013). Anatomy and Human Movement: Structure and Function. Butterworth-Heinemann, Medical. Pages-904.

19. Heimel, J.A., Van Hooser, S.D., Nelson, S.B. (2005). Laminar Organization of Response Properties in Primary Visual Cortex of the Gray Squirrel (Sciurus carolinensis). Journal of Neurophysiology. 4(5): 3538-3554.
20. Yilmaz, G., Ungan, P., Sebik, O., Uginčius, P., Türker, K.S. (2014). Interference of tonic muscle activity on the EEG: a single motor unit study. Front Hum Neurosci. 11; 8:504.
21. Giraudin, A., Cabirol-Pol, M.J., Simmers, J., Morin, D. (2008). Intercostal and abdominal respiratory motoneurons in the neonatal rat spinal cord: spatiotemporal organization and responses to limb afferent stimulation. J Neurophysiol. 99(5):2626-40.
22. Ellaway, P.H., Catley, M., Davey, N.J., Kuppuswamy, A., Strutton, P., Frankel, H.L., *et al*. (2007). Review of physiological motor outcome measures in spinal cord injury using transcranial magnetic stimulation and spinal reflexes. J Rehabil Res Dev. 44 (1):69–76.
23. Ellis H. (2006) Clinical Anatomy: Applied Anatomy for Students and Junior Doctors. Wiley-Blackwell. P-1-456.
24. Wang, K., McGlinn, E.P., Chung, K.C. (2014). A biomechanical and evolutionary perspective on the function of the lumbrical muscle. J Hand Surg Am. 39(1):149-55.